

Lightweight corundum-mullite refractories: I, Effects of pore characteristics and phase compositions on the slag resistance of porous corundum-mullite aggregates

Wen Yan*, Xiaoli Lin, Junfeng Chen, Qingjie Chen and Nan Li

The State Key Laboratory of Refractories and Metallurgy, Wuhan University of Science and Technology, Wuhan, China.

Corrosion of five corundum-mullite aggregates with the same chemical composition and the different pore characteristics and phase compositions by the blast furnace slag were conducted using the static crucible test. Effects of pore characteristics and phase compositions on the slag resistance of the aggregates were investigated through X-ray diffractometer (XRD), scanning electron microscopy (SEM), mercury porosimetry measurement and FactSage[®] software, etc. It is found that the pore characteristics and phase compositions strongly affect the slag resistance of the aggregates. With an increase in apparent porosities (1.4-41.6%), the slag penetration and corrosion resistances of aggregates decrease evidently. When the apparent porosities are in the range of 41.6-44.8%, the pore size plays more important role in the penetration resistance than the viscosity of the slag penetrated; the pore size of 2.74 μm can greatly inhibit the slag penetration. Under the conditions of large difference in the apparent porosities, the phase compositions have little effect on the corrosion resistance; whereas, when the apparent porosities are similar, the higher the corundum content, the higher the corrosion resistance is.

Key words: Lightweight refractories, Porous corundum-mullite aggregates, Slag resistance, Pore characteristics, Phase compositions.

Introduction

Corundum-mullite refractories are widely used for working linings of high temperature vessels, *e.g.*, blast furnaces for iron making, steel ladles for steel making, rotary kilns for iron ore pellet production [1-7]. Generally, these corundum-mullite refractories are manufactured by using dense aggregates as the main raw materials. During the service, the shell temperatures could be high in the high-temperature zones of the high temperature vessels, leading to severe heat loss. To address this issue, it is necessary to develop and use corundum-mullite refractories with lower thermal conductivities, which could be achieved by using porous corundum-mullite aggregates to replace their traditional dense counterparts.

The slag resistance and strength have critical effects on the campaign life of corundum-mullite refractories. Whether the porous corundum-mullite aggregates can replace the dense counterparts depends on their strengths and slag resistances. In our previous research, the porous corundum-mullite ceramics with high strengths and high apparent porosities have been prepared [8-10], so, it is the slag resistance of the porous corundum-mullite aggregates that we should concern about in the present work. Many researches have been done on the slag resistance of the dense

corundum-mullite refractories [2-7]. The slag resistance depends on the microstructure and composition of refractories and the viscosity of slag which may be changed during penetration [11-20]. But, there are not studies on the slag resistances of the porous corundum-mullite refractory aggregates. However, there are some studies on the slag resistance of other refractories with porous structure [13-20]. For example, Mukai et al. had investigated the slag penetration into MgO refractories with different porosity and pore size, and found the rate of slag penetration increased with increasing pore radius and apparent porosity of the refractory [12]; we investigated the corrosion and penetration resistance of porous spinel with small pore size and found that the composition and pore size gave effects on corrosion and penetration resistance of porous spinel refractories [15-20].

Obviously, the slag resistance of porous aggregates could be improved through decreasing the pore size and changing the phase composition. Whereas, when the porous corundum-mullite aggregates all have micro-sizes, the effects of the pore size, apparent porosity and phase composition on the slag resistances of porous corundum-mullite aggregates have not been understood. In order to study the possibility of using the porous corundum-mullite aggregates to fabricate the lightweight refractories for working linings, the corrosion of five corundum-mullite aggregates with the same chemical composition and the different pore characteristics and phase compositions by the blast furnace slag were conducted using the static crucible test, and the effects of pore characteristics and phase

*Corresponding author:
Tel : +86-027-68862511
Fax: +86-027-68862121
E-mail: yanwen@wust.edu.cn

compositions on the slag resistance of the aggregates were investigated in the present work.

Experimental

Five cylindrical blocks having holes of 23 mm in diameter and 18 mm in depth were shaped from a dense corundum-mullite aggregate (DCMA) and four kinds of porous corundum-mullite aggregates (PCMA), respectively. These aggregates have the same chemical compositions, as listed in Table 1. Their apparent porosities and bulk densities were listed in Table 2. The cylindrical blocks were dried at 110 °C for 12 h. 16 g blast furnace slag (Table 1) were placed in the hole in a dried specimen and heated at 1550 °C for 3 h in an electric chamber furnace before furnace-cooling to room temperature.

After the corrosion tests, specimens were cross-sectioned perpendicularly to the slag/refractory interface, as shown in Fig. 1. The actual corroded and penetrated areas in each specimen were measured by the counting pixels method. Corrosion here is defined as the regions of refractory completely replaced by slag. The corrosion index I_C and penetration index I_P are obtained by following equation: $I_{C(P)} = S_{C(P)} / S_0 * 100\%$; S_0 is the original section area of the specimen inner chamber; S_C is the section area of refractory completely replaced by slag; S_P is the penetrated section area.

Apparent porosities were measured based on the Archimedes' principle using water as the medium. Phase identification was carried out by using an X-ray diffractometer (XRD, X'Pert Pro, Philips, Netherlands) with a scanning speed of 2° per minute. Pore size distribution (PSD) and average pore size (APZ) were

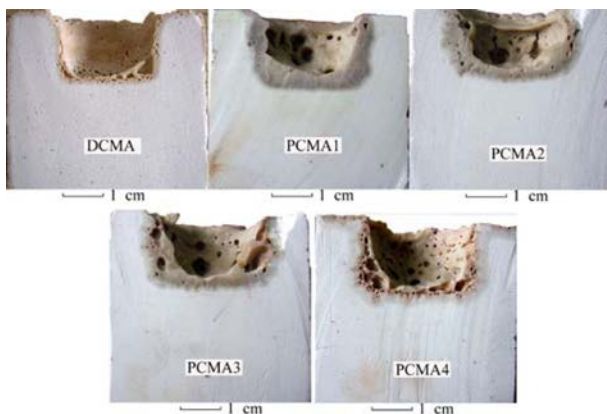


Fig. 1. Photographs of the specimens after the slag test (vertical cut).

measured by a mercury porosimetry measurement (AutoPore IV 9500, Micromeritics Instrument Corporation, USA). Microstructures of these specimens were observed by a field emission scanning electron microscope (FESEM, Nova 400 NanoSEM, FEI Company, USA) equipped with energy dispersive X-ray spectroscopy (EDS, INCA IE 350 PentaFET X-3, Oxford, UK). The viscosities of glass phases at 1550 °C were calculated using the Viscosity Mode of the FactSage® software (version 6.2) based on the EDS results. The dissolution of aggregates into slag were simulated using the Equilibrium Mode of the FactSage® software.

Results and Discussion

Fig. 2 shows the corrosion and penetration indexes of the five specimens corroded for 3h at 1550 °C. For DCMA, PCMA1 and PCMA2, with an increase in apparent porosity (AP) from 1.4 to 42.3%, the penetration and corrosion indexes increase evidently. For PCMA2, PCMA3 and PCMA4 with similar APs (41.6-44.8%), their corrosion indexes are similar, but their penetration indexes are rather different. The penetration index of PCMA4 is much higher than those of PCMA2 and PCMA3.

The slag penetration and corrosion resistances of the aggregates depend on their pore characteristics, chemical and phase compositions, and the reaction between slag and refractories; the latter would affect the dissolution rate of aggregates into slag and the viscosities of slag penetrated. Considering the same chemical composition of the aggregates, the effect of the pore characteristics and phase compositions on slag

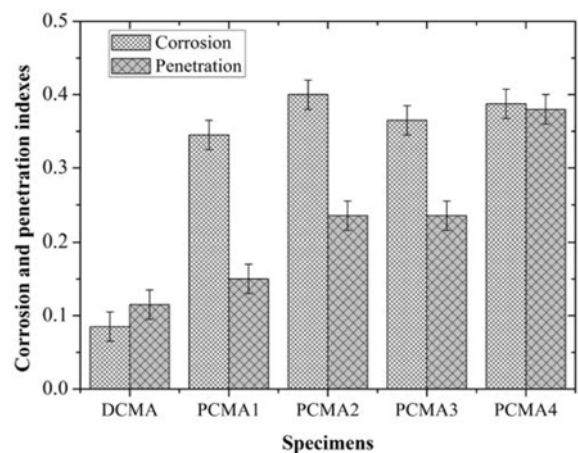


Fig. 2. Corrosion and penetration indexes of the specimens corroded for 3h at 1550°C.

Table 1. Chemical compositions of aggregates and slag (wt%).

	SiO ₂	Al ₂ O ₃	Fe ₂ O ₃	CaO	MgO	K ₂ O	Na ₂ O	Ti ₂ O	MnO
Aggregates	19.38	79.89	0.18	0.07	0.06	0.05	0.18	0.19	–
Slag	31.50	16.08	0.75	40.17	9.92	–	–	0.81	0.40

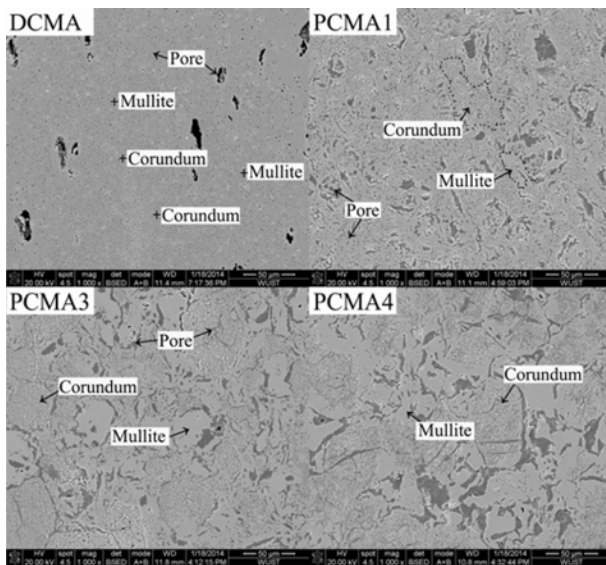


Fig. 3. Microstructures of DCMA, PCMA1, PCMA3 and PCMA4.

Table 2. Apparent porosities, bulk densities and average pore sizes of aggregates.

	DCMA	PCMA1	PCMA2	PCMA3	PCMA4
Apparent porosity (%)	1.4	31.6	41.6	42.3	44.8
Bulk density (g/cm ³)	3.18	2.28	1.96	1.94	1.86
Average pore size (μm)	1.40	3.41	3.16	2.74	5.64

Error ranges of apparent porosity, bulk density and APZ are ± 1.0 , ± 0.02 and ± 0.05 , respectively.

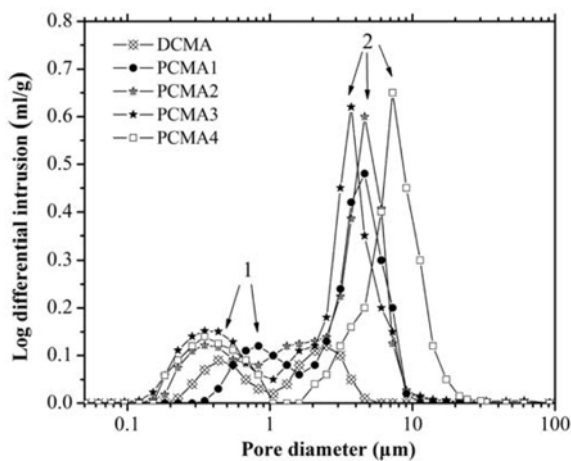


Fig. 4. Pore size distributions of the five corundum-mullite aggregates.

resistance will be the focus in the later discussion.

The slag penetration resistance depends on the AP, average pore size (APZ), and the viscosities of slag penetrated. Pores are the main channel for the penetration of the slag. The less the porosity and the pore size, the higher the penetration resistance is. The

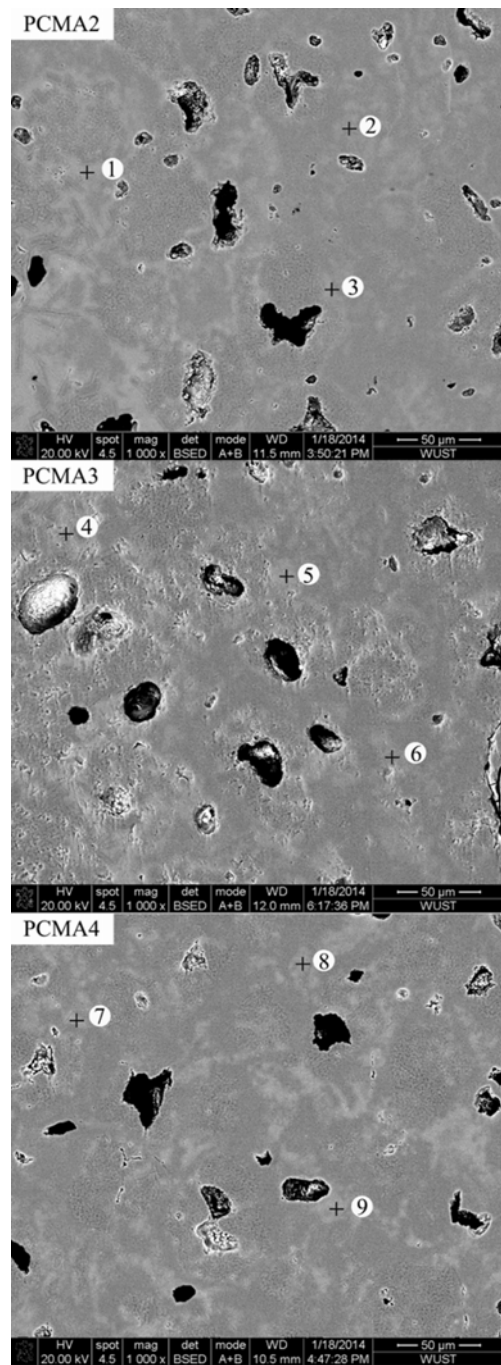
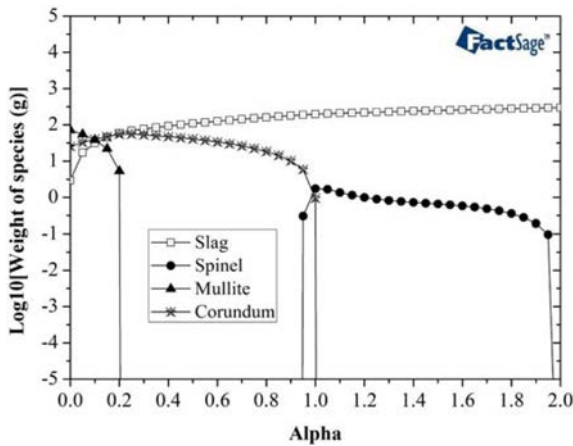


Fig. 5. Microstructures of penetration layers of PCMA2, PCMA3 and PCMA4.

microstructures and pore size distributions (PSDs) of the aggregates are shown in Fig. 3 and Fig. 4, respectively. All aggregates consist of two types of pores (Fig. 3) and the bi-peak modes of the PSDs are observed in all the aggregates (Fig. 4). Their APZs of aggregates are shown in Table 2. For DCMA, PCMA1 and PCMA2, DCMA has the highest penetration resistance because it has the smallest AP and APZ; whereas, comparing with PCMA1 with PCMA2, the penetration resistance of PCMA1 is greatly higher than that of PCMA2, because the former has the lower AP.

Table 3. EDS results and viscosities at 1550 °C of glass phases in Fig. 5.

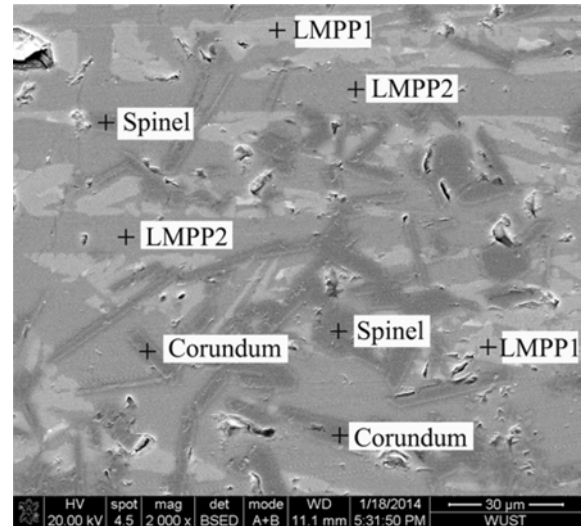
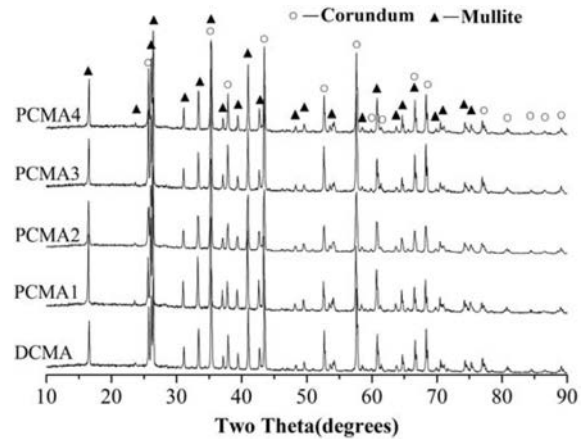
		1	2	3	4	5	6	7	8	9
EDS results (wt%)	Al ₂ O ₃	32.79	33.64	30.92	38.56	38.09	36.12	39.39	33.14	32.29
	SiO ₂	50.54	52.52	54.49	47.35	47.83	49.69	49.24	52.84	51.55
	CaO	16.67	13.83	14.60	14.10	14.08	14.19	11.37	14.03	16.15
Viscosities (Pa · S)		7.17	11.79	15.24	5.13	5.53	7.37	7.25	12.25	8.66
Average values of viscosities (Pa · S)			11.40			6.01			9.39	

**Fig. 6.** Relationship between the weight of the predicated species and alpha value.

For PCMA2, PCMA3 and PCMA4, PCMA4 has the lowest slag penetration resistance because of its largest AP and APZ; whereas, PCMA2 and PCMA3 have similar slag penetration resistance, which may relate with the viscosity of the penetrated slag, because they have similar APs and different APZs.

The microstructures of the penetration layers of PCMA2, PCMA3 and PCMA4 are given in Fig. 5. The bright contrast phases (referred to as 1 to 9) in Fig. 5 are glass phases whose EDS results are listed in Table 3. They mainly consist of Al₂O₃, SiO₂ and CaO. The Al₂O₃, SiO₂ and CaO contents of glass phases in the penetration layers are different. Consequently, the viscosities of the penetrated slags in PCMA2 are higher than those in PCMA3 and PCMA4. The higher the viscosity of the slag, the more difficult the penetration of the slag is. Although the viscosities of the slag penetrated in PCMA4 is higher than those in PCMA3, both the larger APs and APZs result in the lowest penetration resistance of PCMA4. The similar slag penetration resistances of PCMA2 and PCMA3 means that the small pore size of PCMA3 is more effective to improve the slag penetration resistance than the viscosities of penetrated slag in the present work, because they have similar APs.

The slag corrosion resistance depends on the dissolution rate of aggregates into slag which can be explained through the thermodynamic calculation conducted with the FactSage[®] package, and the contact area between the slag and aggregates. Fig. 6 shows the

**Fig. 7.** Microstructure of reaction layer of PCMA1, Low melting-point phase 1 (LMPP1) consists of 30.41-32.38 wt% Al₂O₃, 29.61-33.48 wt% SiO₂ and 36.10-38.02 wt% CaO, LMPP2 consists of 34.33-35.62 wt% Al₂O₃, 45.85-46.91 wt% SiO₂ and 18.43-18.85 wt% CaO.**Fig. 8.** XRD patterns of aggregates.

relation between the weight of the predicated species and alpha value at 1550 °C according to the chemical compositions of aggregates and slag listed in Table 1. For alpha = 2, the calculations were carried out with 100 g aggregates and 200 g slag. At alpha value of 0, the theoretical phase contents of the five aggregates are 71.70 wt% mullite, 25.36 wt% corundum and 2.94 wt% slag. With an increase in alpha value the weight of mullite and corundum decreases and abruptly

Table 4. Relative phase contents of aggregates (wt%).

	DCMA	PCMA1	PCMA2	PCMA3	PCMA4
Corundum	28	31	32	39	34
Mullite	72	69	68	61	66

drops to zero at alpha of 0.20 and 1.00, respectively. At alpha value of 0.94, spinel is formed, and at alpha value of 1.96, the weight of spinel drops to zero. It means that the dissolution rate of mullite into slag is much higher than that of corundum, and spinel will be formed after the dissolution of aggregate into slag. A typical microstructure of reaction layer of PCMA1 is given in Fig. 7. Only corundum, spinel and low melting-point phases are found, because mullite has been dissolved into slag in the layer, which verifies the simulation results shown in Fig. 6. So, a conclusion could be obtained, that is, the higher the content of mullite in aggregate, the lower the corrosion resistance is.

XRD patterns of aggregates are shown in Fig. 8 and the relative phase contents of aggregates are listed in Table 4. In all aggregates, the phases are corundum and mullite. From DCMA to PCMA2, although the content of mullite in DCMA is the highest, the lowest AP results in the smallest contact area between the slag and aggregate, which lead to the slowest dissolution rate. It is the main reason why DCMA shows better slag corrosion resistance than others. For PCMA2, PCMA3 and PCMA4, their similar APs result in the similar contact areas between the slag and aggregates, and thus the phase compositions play more important role in the corrosion resistance. Among these three aggregates, PCMA 2 has the highest mullite content, lead to the lowest corrosion resistance, whereas, PCMA3 has the lowest mullite content, and thus has the highest corrosion resistance. Additionally, the viscosities of the penetrated slag are affected by the mullite content in the aggregate; the higher content of mullite in aggregate results in the higher SiO₂ content in the slag penetrated, which makes the increase of the viscosities of the slag penetrated, it is accordant with the results shown in Fig. 5 and Table 3.

Obviously, comparing with the dense corundum-mullite aggregate, the slag resistance of the lightweight aggregate deteriorates. Whereas, when the dense corundum-mullite aggregates were substituted by the porous in the refractories, how the porous aggregates affect the slag resistance of the lightweight corundum-mullite refractories has not been understood. It will be discussed in our another work [21].

Conclusions

Corrosion of five corundum-mullite aggregates with the same chemical composition and the different pore

characteristics and phase compositions by blast furnace slag were conducted using the static crucible test. It is found that pore characteristics and phase compositions strongly affect the slag resistance of the aggregates.

With an increase in AP (1.4-41.6%), the slag penetration and corrosion resistances of aggregates decrease evidently. When the APs are in the range of 41.6-44.8%, the pore size plays more important role in the penetration resistance than the viscosity of the slag penetrated; the pore size of 2.74 μm can greatly inhibit the penetration of slag.

When the difference among the APs is evident, the phase composition has little effect on the corrosion resistance; whereas, when the APs are similar, the higher the corundum content, the higher the corrosion resistance is.

Acknowledgments

The authors would like to thank the Educational Commission of Hubei Province of China (Grant No. Q20131111) and the Science Foundation of the State Key Laboratory of Refractories and Metallurgy of China (Grant No. 2014QN01) for financially supporting this work.

References

1. C. Aksel, *Ceram. Int.* 29 (2003) 183-188.
2. B. Meng, J. Peng, *Ceram. Int.* 39 (2013) 1525-1531.
3. J. Stjernberg, M.A. Olivas-Ogaz, M.L. Antti, J.C. Ion, B. Lindblom, *Ceram. Int.* 39 (2013) 791-800.
4. J. Liu, *Refractories & Lime* 34 (2009) 33-36.
5. L. Wang, Z. Li, J. Sun, D. Zhang, X. Li, *Ironmaking* 20 (2001) 31-32.
6. P. Duan, X. Hu, X. Xue, J. Li, *Journal of Northeastern University (Natural Science)* 19 (1998) 60-63.
7. X. Xue, X. Hu, P. Duan, *Naihuo Cailiao* 32 (1998) 136-137.
8. W. Yan, N. Li, *Am. Ceram. Soc. Bull.* 85 (2006) 9401-9406.
9. W. Yan, N. Li, B.Q. Han, *J. Ceram. Process. Res.* 11 (2010) 388-391.
10. S.J. Li, N. Li, *Ceram. Int.* 33 (2007) 551-556.
11. W.E. Lee, S. Zhang, *Int. Mater. Rev.* 44 (1999) 77-104.
12. K. Mukai, Z.N. Tao, K. Goto, Z.S. Li, T. Takashima, *Scand. J. Metall.* 31 (2002) 68-78.
13. H.Z. Gu, L.P. Fu, L.Y. Ma, *Interceram* 3 (2014) 121-124.
14. L.P. Fu, H.Z. Gu, A. Huang, M.J. Zhang, X.Q. Hong, L.W. Jin, *Ceram. Int.* 41 (2015) 1263-1270.
15. W. Yan, N. Li, B.Q. Han, *Sci. Sinter.* 41 (2009) 275-281.
16. W. Yan, N. Li, B.Q. Han, X.M. Fang, G.P. Liu, *Ceram-Silikáty* 54 (2010) 315-319.
17. W. Yan, N. Li, Z. Miao, G.P. Liu, Y.Y. Li, *J. Ceram. Process. Res.* 13 (2012) 278-282.
18. W. Yan, N. Li, B.Q. Han, *Int. J. Appl. Ceram. Tec.* 5 (2008) 633-640.
19. W. Yan, N. Li, B.Q. Han, *Interceram* (2009) 25-28.
20. W. Yan, N. Li, *Proceedings of the Fifth International Symposium on Refractories* (2007) 215-219.
21. W. Yan, Q.J. Chen, X.L. Lin, J.F. Chen, N. Li, *J. Ceram. Process. Res.* submitted.